PAPER • OPEN ACCESS

Vortex generator's effect on trailing edge vortex shedding and fluid structure interaction

View the article online for updates and enhancements.

Vortex generator's effect on trailing edge vortex shedding and fluid structure interaction

H Besirovic, K F Sagmo, P T Storli

Waterpower Laboratory, NTNU, NO-7491, Alfred Getz Vei 4, Trondheim

E-mail: `HasanB@stud.ntnu.no`

Abstract. An initial study of the effects vortex generators (VGs) have on the mitigation of vortex-induced vibrations (VIVs) of hydrofoils have been performed at the Waterpower laboratory of the Norwegian University of Science and Technology. The VGs are placed close to the trailing edge of a blunt hydrofoil. Reasonable design parameters of the VGs were found from the literature with regard to which would induce the strongest vortices with the lowest drag. Vibration frequencies of the hydrofoil were measured using flush mounted strain gauges located close to the trailing edge. This paper presents the design of the VGs and some initial results of the experiments performed with these devices. The preliminary results indicate a possible mitigation of VIVs. This could be because of the interference between the primary vortices generated by the hydrofoil and the longitudinal vortices generated by the VGs, but further work is necessary to make a conclusion.

1. Introduction

As the demand for energy is increasing every day, it is important to look at ways of making the process of producing and utilising energy as cost-efficient as possible. Avoiding unnecessary wear and the risk of failure is thus important. Devices put in a flow tend to experience vibrations known as vortex-induced vibrations (VIVs). When such vibrations approach the natural frequency of such devices, resonance, inducing wear and failure may occur. Examples of such devices can be stay vanes in hydropower plants, rudders in ships as well as wind and water power turbine blades. As a means of studying the mitigation of these VIVs, it has been proposed to attach vortex generators (VGs) at the trailing edge of a simple hydrofoil. The goal with these VGs is to generate strong longitudinal vortices which can interfere with the uniformity of the Kármán vortex street, which is formed in the wake of the hydrofoil. VGs were first introduced by Taylor in 1947 [1]. Since then several parametric studies have been conducted on similar devices by researchers like Lin [2], Kundu et al [3] and Godard and Stanislas [4]. So far VGs have most commonly been used to control flow separation and used extensively in the aircraft industry in order to increase the stall angle of aeroplanes. Although the phenomena of controlling flow separation are most studied, Holmes et al. [5] have shown that in addition to delaying separation the VGs are able to break up the vortex street thus possibly mitigating the VIVs. Even though VGs have mostly been studied with air as the fluid, some papers where VGs have been studied in a hydrodynamic setting have been found. Brandner and Walker [6] have looked at hydrodynamic applications and especially the effects of cavitation on VGs. Their results show that application of VGs with an appropriate angle of attack and in pressurised

systems can help avoid cavitation. This is opening up the possibilities for such devices to be used in hydrodynamic systems.

2. Experimental overview
2.1. Vortex Generators
The dimensions of the VGs and thus the design, shown in figure 1 were based on research done on these devices. The main papers that inspired the design of the VGs were Lin [2], Brandner and Walker [6] and Kundu et al. [3]. The VGs were placed in a counter-rotating (CoR) configuration because this has been proven to be the most effective when looking at the lift to drag ratio and produce the stronger vortices. VGs in this orientation tend to produce vortices which diffuse less downstream in addition to producing vortex strengths twice that of other configurations [4]. In order to have VGs with low induced drag and strong vortices that most effectively energise the boundary layer, a triangular shape was chosen. Mueller-Vahl et al. [7] also showed that vortex generators with too large height would lead to early lift-off of vortices from the surface. For these reasons a height, $h = 1.92$, of a fraction of the boundary layer height, $h \approx 0.3\delta_{99}$ was chosen. Note that here the boundary layer thickness δ_{99} at the position of the VGs was estimated from the Reynolds Average Navier Stokes (RANS) simulations of the same case recently presented by Sagmo and Storli [8]. The other parameters shown in figure 1 were chosen such that they were proportional to the VG height (h).
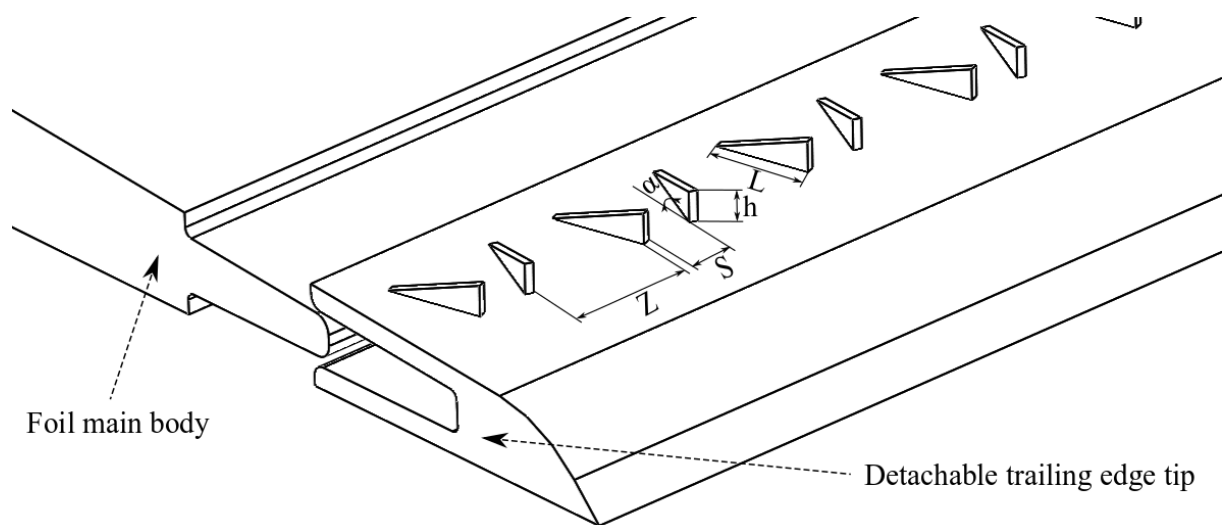

Figure 1. Trailing edge tip attachment mechanism and VG parameters

The length, L, was chosen to be $L = 3h$, which was believed to be a good trade-off when looking at the drag increase longer VGs entail. The VGs were positioned (Lengthwise Position (LP), figure 2) such that the trailing edge of the devices were $5h$ upstream of the point of separation found in [9]. A span-width, S, between the counter-rotating VGs was set because it has been shown that the decay of vortices downstream is an order of magnitude lower when compared to VGs with zero span-width [2]. A span of $S = 1.5h$ was chosen. The spacing between adjacent VG pairs were set to be $Z = 2.5h$. This is in order to most effectively energise the boundary layer while having the highest lift to drag ratio. It is a rough average of the optimal values found by Betterton [10], Godard and Stanislas [4] and Mueller-Vahl et al [7]. Then the angle, $\alpha = 20°$, was chosen based on the results of Brandner and Walker [6], Pauley and Eaton [11], Godard and Stanislas [4] and Raykowski [12]. All the dimensions of the VGs are summarised in table 1.

Table 1. Final dimensions of the VGs

Configuration	h	L/h	Z/h	S/h	α	LP/h
CoR	1.92mm	3	2.5	1.5	20°	5

2.2. Hydrofoil

The hydrofoil geometry is shown in figure 2. Trailing edge thickness at the position where the curve starts is $D = 4.8mm$ and is used as the characteristic length. The hydrofoil is compromised of two parts, as seen in figure 1. It shows a cut section view of the hydrofoil studied with a detachable trailing edge (TE). This is made such that several different TEs can be tested. The trailing edge tip is attached with a though, Valtron two-component epoxy heat release glue, the Valtron AD4010, manufactured by Valthech Corp. The glue expands and releases at temperatures over $90°Celsius$ for easy removal. The foil was machined from a block of aluminium alloy and coated with a thin matte black paint. The black paint serves two purposes, to make a flush hydraulically smooth glue joint as well as to reduce laser reflections for the potential use of Particle image velocimetry (PIV).
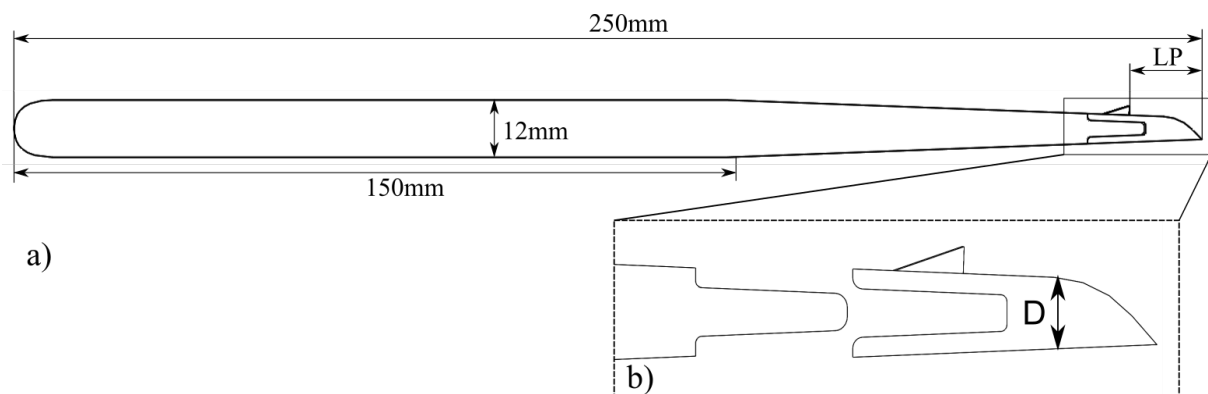

Figure 2. a) Overall dimensions of hydrofoil. b) Attachment mechanism for an interchangeable trailing edge.

2.3. Experimental procedure

All measurements are done with the hydrofoil at an 0° angle of attack. The set-up is illustrated in figure 3. Volumetric flow rate is measured using an ABB electromagnetic flow-meter calibrated up to a volumetric flow of $0.4m^3/s$ located downstream of the hydrofoil. An RTD PT100 thin film, 4-wire temperature sensor is also located downstream of the test section to measure water temperature variations. Vibration frequencies of the hydrofoil were measured using two strain gauges from Kulite, flush mounted in a half-brige configuration, located $\approx 11.5D$ from the trailing edge of the hydrofoil.

Data attainment was managed by Lab-VIEW and National Instruments (NI) data acquisition devices (DAQ's). The sampling rate was set to 25kHz in order to have at least 25 samples per period for the shedding frequencies investigated. Amplitude spectrum was obtained using P.D Welch's power spectrum method in Python with a Hanning window and a segment overlap of 50%. A Kaiser window was used for especially noisy data and with data with two frequencies
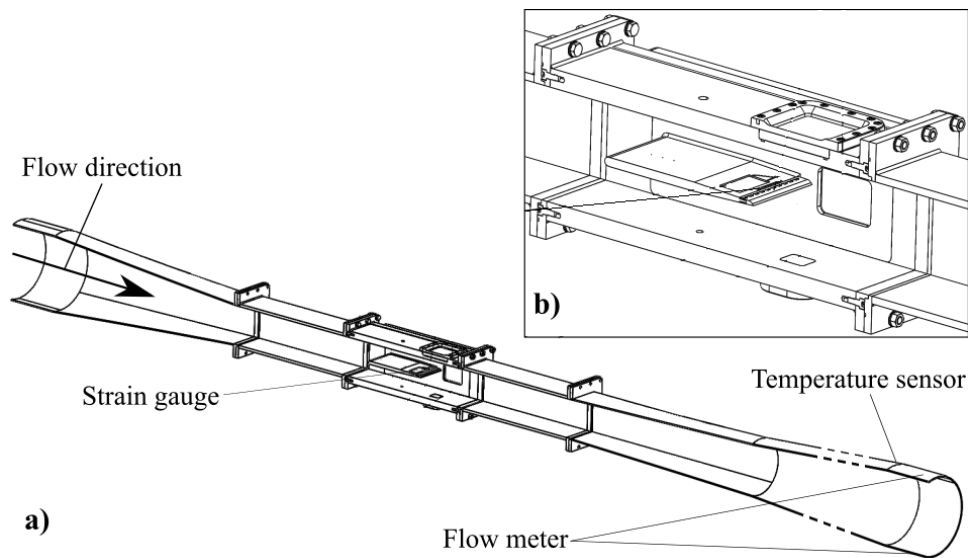
Figure 3. a) View of the experimental set up. b) An enlarged view of the test section with the hydrofoil and VGs.

of interest close to each other. For the current preliminary analysis the trailing edge vortex shedding is estimated empirically with the Strouhal shedding frequency given by equation 1, where the Strouhal number is obtained from the measurements in [9] of a identical hydrofoil profile without VGs, and is $St = 0.274$. Note that this result is based on the reference velocity, U_{ref} set equal to the test section bulk velocity.

$$f_s = \frac{St \cdot U_{ref}}{L} \tag{1}$$

3. Experimental results

Figure 4 shows vibration frequencies obtained by means of the strain gauges near the trailing edge of the hydrofoil. The estimated Strouhal shedding frequency based on the aforementioned strouhal number of 0.274 is also plotted with a dashed line over the range of test section flow velocities. The maximum amplitude of the foil vibrations correspond well to the overlapping of the estimated shedding frequency and the natural frequency of the foil. The standing peak in the strain gauge frequency-amplitude spectrum shown in figure 5 can be identified as the natural frequency of the hydrofoil. A value of $\approx 622 Hz$ agrees well with the natural frequency found in [9] indicating that the natural frequency of the hydrofoil does not change significantly with the attachment of VGs.

4. Conclusion/Discussion

Notably, as shown in figure 4 there is only a relatively slow rise in the trailing edge vibrational amplitude at the intersection of the estimated shedding frequency and the eigenfrequency of the foil compared to the previous results obtained for the same trailing edge profile without the VGs [9]. This could indicate that the shedding frequency never fully synchronises up with the natural frequency of the hydrofoil, though it is unclear at the present point how much of the dampening effect is due to the VGs and how much may be due to an effect of the trailing edge glue joint. In figure 5, a) we observe what seem to be a group of exited frequencies around 270 Hz closely corresponding to the estimated shedding frequencies. For low velocities, the group tends to travel towards the natural frequency but is relatively suppressed at higher velocities compared
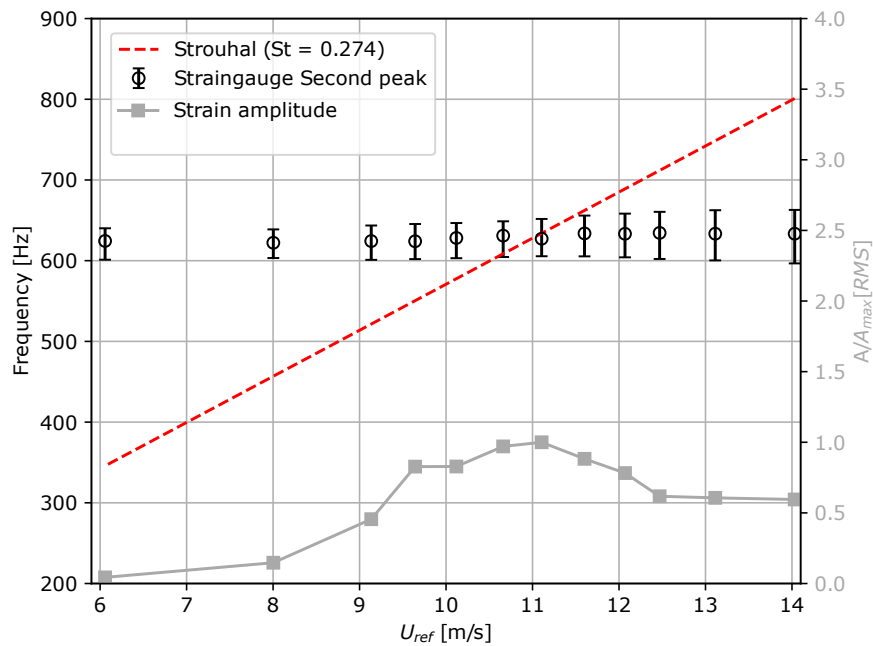
Figure 4. Vibration frequencies measured by the means of a strain gauge plotted on the left axis. Relative strain amplitude of the hydrofoil vibrations plotted on the right axis.
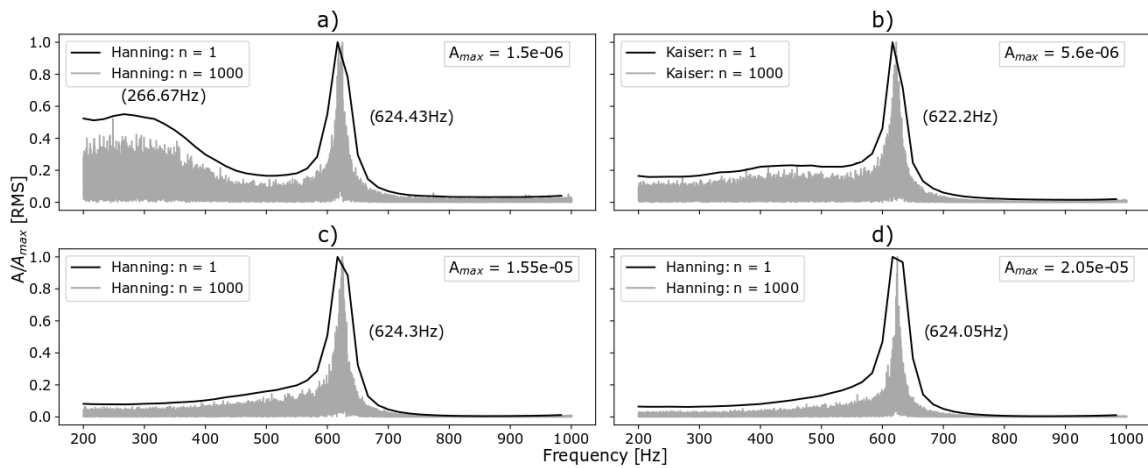

Figure 5. Amplitude frequency spektrum obtained by means of P.D Welch power spektrum and a Hanning or Kaiser window. a) $U_{ref} = 6.0\frac{m}{s}$. b) $U_{ref} = 8.0\frac{m}{s}$. c) $U_{ref} = 9.1\frac{m}{s}$. d) $U_{ref} = 9.6\frac{m}{s}$.

to the clear peak at the hydrofoil's natural frequency. This is in contrast to the results in [9] for the same trailing edge shape without VGs, where the shedding frequencies can be clearly tracked in the strain signal well into the VIV interference region. These results are indicative of a weakened state of vortex shedding, possibly due to a interference between the streamwise vortices generated by the VGs and the Kármán vortex street. However it is essential to take into consideration that only a few sets of data were obtained for this hydrofoil configuration

with VGs with the means of strain gauges. While interesting, the data is therefore believed to be insufficient to draw a conclusion on the effects VGs have on mitigating the vortex induced vibrations. Further work is required.

5. Further Work

Further work will involve a analysis of the wake and shedding shedding frequency using PIV. A more detailed study around the velocities where the shedding frequency seems to be suppressed with smaller velocity increments than present for each measurement point should be performed. This is in order to detect if a state of lock-in was skipped due to too large velocity increments. A set of measurements will also be conducted on the hydrofoil with the exchangeable trailing edge tip without VGs in order to be able to quantify the effects on the results of the glue joint for the attachment mechanism.

References

[1] Taylor H D 1947 *United Aircraft Corporation, East Hartford, CT, Technical Report No* **4012** 3
[2] Lin J C 2002 *Progress in Aerospace Sciences* **38** 389–420 ISSN 03760421 URL https://linkinghub.elsevier.com/retrieve/pii/S0376042102000106
[3] Kundu P, Sarkar A and Nagarajan V 2019 *Renewable Energy* **142** 643–657 ISSN 09601481 URL https://linkinghub.elsevier.com/retrieve/pii/S0960148119306329
[4] Godard G and Stanislas M 2006 *Aerospace Science and Technology* **10** 181–191 ISSN 12709638 URL https://linkinghub.elsevier.com/retrieve/pii/S127096380500163X
[5] HOLMES A, HICKEY P, MURPHY W and HILTON D 1987 *25th AIAA Aerospace Sciences Meeting* p 84
[6] Brandner P and Walker G 2003 *Experimental Thermal and Fluid Science* **27** 573–582 ISSN 08941777 URL https://linkinghub.elsevier.com/retrieve/pii/S0894177702002716
[7] Mueller-Vahl H, Pechlivanoglou G, Nayeri C N and Paschereit C O 2012 *Volume 6: Oil and Gas Applications; Concentrating Solar Power Plants; Steam Turbines; Wind Energy* (Copenhagen, Denmark: American Society of Mechanical Engineers) pp 899–914 ISBN 978-0-7918-4472-4
[8] Sagmo K F and Storli P T 2019 *Journal of Physics: Conference Series* **1296** 012004
[9] Sagmo K F, Tengs E O, Bergan C W and Storli P T 2019 *IOP Conference Series: Earth and Environmental Science* **240** 062006 ISSN 1755-1315 URL http://stacks.iop.org/1755-1315/240/i=6/a=062006?key=crossref.f4c2e714e42d5380fd024883c71f86ec
[10] Betterton J G, Hackett K C, Ashill P R, Wilson M J, Woodcock I J, Tilman C P and Langan K J 13
[11] Pauley W R and Eaton J K 1988 *AIAA Journal* **26** 816–823 ISSN 0001-1452, 1533-385X URL https://arc.aiaa.org/doi/10.2514/3.9974
[12] Raykowski K A 1999 *Optimization of a Vortex Generator Configuration for a 1/4-Scale Piper Cherokee Wing* Master's thesis Embry-Riddle Aeronautical University